Nuclear Relaxation in Aluminum*

JOHN J. SPOKAS† AND CHARLES P. SLICHTER‡
Department of Physics, University of Illinois, Urbana, Illinois
(Received November 3, 1958)

Nuclear spin-lattice relaxation times T_1 and phase memory times T_2 have been measured in 99.99% pure aluminum foil from 77°K to the melting point by the spin-echo method. At high temperature the line narrows due to self-diffusion, as previously observed by Seymour. The temperature dependence of the narrowing gives an activation energy of self-diffusion E_D of 1.4±0.1 ev. From the measured "narrowing temperature" and Nowick's theoretical estimate of D_0, the same value of E_D is found. As predicted theoretically, measurements show that T_1 arises from interaction with conduction electrons and is inversely proportional to temperature from 1°K to 930°K. At the highest temperatures, an unknown line broadening mechanism is found which is believed to represent quadrupole coupling to strain fields of dislocations. The measurements were made feasible only through the use of a phase-coherent detection sytem, a description of which is given.

I. INTRODUCTION

NUCLEAR magnetic relaxation times are profoundly affected by atomic and molecular motions. The characteristic frequencies of atomic diffusion are often sufficiently rapid even in the solid phase to modify the line width. If the magnetic dipole interaction between nuclei dominates the line breadth, information can then be obtained concerning the diffusion process. Holcomb and Norberg[1] have experimentally determined the self-diffusion coefficients of lithium and sodium by magnetic resonance. The nuclear resonance of aluminum is also expected to exhibit diffusion effects the analysis of which should permit a determination of the self-diffusion constant. The conventional tracer methods have not yet been applied to aluminum owing to the lack of a suitably long-lived isotope. However, Nowick[2] has predicted that reasonable values for D_0 and E appearing in the expression $D=D_0\exp(-E/kT)$ for the diffusion coefficient are 0.45 cm²/sec and $E=1.43$ ev. Seymour[3] has already reported the abrupt narrowing of the aluminum nuclear resonance near 300°C, which he attributes to diffusion and from which he determines $D_0=10^{-3\pm1}$ cm²/sec and $E\simeq0.9$ ev. However, as we shall discuss in Sec. II, the "narrowing temperature" indicated by Seymour's data gives $E\simeq1.4$ ev. By employing a pulse magnetic resonance apparatus which uses phase coherent detection, we have been able to extend Seymour's measurements greatly. The nuclear spin relaxation time T_1 and phase-memory time T_2 have been determined up to the melting point, 660°C. The activation energy for self-diffusion obtained from the temperature dependence of the line narrowing as determined in this research is 1.4±0.1 ev. Above 500°C, the line breadth is no longer dominated by the nuclear dipole couplings, reminiscent of the cases of lithium and sodium where an extra broadening mechanism was also found. The spin-lattice relaxation times, T_1, measured in this research together with low-temperature determinations of other workers are inversely proportional to the absolute temperature from 1°K to about 1000°K as expected for relaxation via the conduction electrons. The data are represented by $T_1T=1.85\pm0.05$ sec-°K.

The results anticipated for aluminum are discussed in the next section. The relevant features of the phase coherent apparatus and the experimental methods employed are discussed in Sec. III. The experimental results and interpretation are presented in Sec. IV.

II. THEORY OF TEMPERATURE DEPENDENCE OF LINE WIDTH

Natural aluminum consists of the single isotope Al^{27} which possesses a spin $I=\frac{5}{2}$ with accompanying gyromagnetic ratio $\gamma/2\pi=11.1\times10^2$ (sec oersted)$^{-1}$ and electric quadrupole moment $Q=+0.156\times10^{-24}$ cm².[4] Since the aluminum lattice is face-centered cubic, electric quadrupole interactions vanish unless the crystalline symmetry is disturbed by some kind of imperfection. Therefore, quadrupole effects will be omitted in the present discussion although evidence will be presented in Sec. IV which supports the view that the high-temperature data manifests a quadrupole interaction. Exclusive of possible quadrupole effects, the interaction with neighboring nuclei and with the conduction electrons is expected to account for the characteristics of the aluminum resonance completely.

Both the observed line widths and the observed spin-lattice relaxation times, T_1, are in general determined by the combined effect of several processes. We assume that the observed spin-lattice relaxation *rate*, $1/T_1$, is simply the sum of the rates due to the separate processes. For our purposes it is most convenient to characterize line widths by specifying the phase memory time, T_2. Several definitions of T_2 appear in the literature. Our definition will be given in a later

* This research supported in part by a grant from the Office of Naval Research and in part by a grant from the Alfred P. Sloan Foundation.
† Now at the RCA Laboratories, Princeton, New Jersey.
‡ Alfred P. Sloan Fellow.
[1] D. F. Holcomb and R. E. Norberg, Phys. Rev. **98**, 1074 (1955).
[2] A. S. Nowick, J. Appl. Phys. **22**, 1182 (1951).
[3] E. F. W. Seymour, Proc. Phys. Soc. (London) **A66**, 85 (1953).
[4] Hin Lew, Phys. Rev. **76**, 1086 (1949).

part of the paper, but at this stage we may remark that $1/T_2$ characterizes some sort of width. At sufficiently high temperatures, our lines have Lorentzian shape. We shall assume that when the line width results from more than one process, all processes give Lorentzian shapes by themselves, and that the reciprocal of the observed T_2 is the sum of the reciprocals of the T_2's from each process.

For a Lorentzian line, the line width produced by a *single* interaction (the kth such interaction) can be written as the sum of two terms:

$$(1/T_2)_k=(1/T_2')_k+(1/T_1')_k. \tag{1}$$

The first term on the right, called the secular term, arises from those matrix elements of the perturbation which are diagonal in the nuclear Zeeman representation. The nonsecular term $1/T_1'$ results from processes which require an exchange of energy between the nuclear spins and their surroundings. The nonsecular term never exceeds the corresponding thermal relaxation rate, $1/T_1$. The significance of the two types of broadening has been discussed in the literature.[5,6]

The dominant coupling to the conduction electrons is via the magnetic interaction with their spin magnetic moments, through the so-called Fermi interaction.[7] This coupling provides both a paramagnetic shift of the nuclear resonance frequency, the Knight shift, and a strong thermal relaxation mechanism. We are only concerned with the thermal relaxation and the accompanying line breadth contribution. It has been shown[1,7] that $(T_2)_{\text{elec}}=(T_1)_{\text{elec}}$, and that both are inversely proportional to the absolute temperature. Redfield[8] has observed $T_1\simeq 6$ msec in aluminum at room temperature in reasonable agreement with theoretical expectations. In addition, his low-temperature measurements[9] fit an inverse temperature dependence. Excluding other relaxation mechanisms we anticipate $T_1\simeq 2$ msec near the melting point.

Low-temperature line widths in solids are usually broad (of order several gauss) and independent of temperature. The broad resonances observed in most solids can often be completely accounted for in terms of the local field produced at one nucleus by the neighboring nuclear moments, μ. For a neighbor a distance r away, the dipolar field is approximately μ/r^3, yielding a field of order one gauss for the nearest neighbor separation in aluminum. A precise description of the dipolar interaction is provided by Van Vleck's theory of the second moment.[10] The value calculated for aluminum is $\langle\Delta H^2\rangle=7.63$ gauss^2 which is to be compared with the average of published room-temperature values 10 ± 1 gauss^2.[11,3,8] This discrepancy is perhaps not significant since second-moment measurements are very difficult. The important fact to note is that the room-temperature relaxation rate $1/T_1\simeq 170$ sec^{-1} contributes negligibly to the line breadth $1/T_2\simeq 22\,000$ sec^{-1}.

The dipolar broadening of the nuclear resonance can be greatly diminished at elevated temperatures by the increased rapidity of atomic motions. In particular, the motion of atomic diffusion can drastically alter the line breadth in solids. The explanation of motional narrowing was given by Bloembergen, Pound, and Purcell[5] who described it by a one-parameter "noise theory." Their result, which has proven exceedingly helpful in understanding much resonance data, is

$$(1/T_2')^2=(2/\pi)(\delta\omega_0)^2\tan^{-1}(2\tau/T_2'), \tag{2}$$

where $(1/T_2')$ is the secular line-width contribution, τ is the so-called correlation time describing the time-varying field, and $\delta\omega_0$ is the rigid lattice breadth in frequency. As a function of τ, Eq. (2) predicts two limiting dependences; for $\tau\delta\omega_0\gg 1$ the secular width is constant, and for $\tau\delta\omega\ll 1$ the secular width is proportional to the correlation time. An important feature of Eq. (2), of which use will be made below, is that the transition between the two cases is relatively sharp. The transition region spans approximately two orders of variation in τ whereas the total range of τ observed in an experiment may cover many factors of ten.

It is often true that a pronounced change in line shape accompanies the narrowing phenomenon. Although a variety of shapes are found in the rigid lattice depending on such effects as crystal structure and orientation, lines become essentially Lorentzian when narrowed. The theory of the shape of the rigid lattice line has not been worked out for any but a few special cases. The Lorentzian shape of the narrowed lines has been explained. It is evident, therefore, that we must not treat Eq. (2) as being precise, encompassing as it does *all* cases of line width. Rather we should look on it as giving a semiquantitative description of the narrowing phenomenon. Kubo and Tomita[6] have examined in detail the general problem of narrowing in magnetic resonance. They have obtained the BPP expression for all values of τ for the particular model in which the rigid lattice shape is Gaussian and where $1/T_2'$ is defined as the half-power width.

The correlation time for the dipolar interaction is proportional to the mean time between elementary jumps of the diffusion process as has been shown by Bloembergen, Purcell, and Pound.[5] Random-walk diffusion theory[12] relates the jump time to the diffusion coefficient for a vacancy mechanism in an fcc lattice according to

$$\tau=a^2/12D, \tag{3}$$

[5] Bloembergen, Pound, and Purcell, Phys. Rev. **73**, 679 (1947); hereafter referred to as BPP.
[6] R. Kubo and K. Tomita, J. Phys. Soc. (Japan) **9**, 888 (1954).
[7] J. Korringa, Physica **16**, 601 (1950).
[8] A. G. Redfield, Phys. Rev. **98**, 1787 (1955).
[9] A. G. Redfield, Phys. Rev. **101**, 67 (1956).
[10] J. H. VanVleck, Phys. Rev. **74**, 1168 (1948).
[11] H. S. Gutowsky and B. R. McGarvey, J. Chem. Phys. **20**, 1472 (1952).
[12] C. Zener, J. Appl. Phys. **22**, 372 (1951).

in which a is the lattice constant and D the diffusion coefficient. Furthermore D should satisfy the Arrhenius relation

$$D=D_0 \exp[-E_D/kT], \quad (4)$$

where D_0 and E_D, the activation energy, are independent of temperature and k is Boltzmann's constant. From Eqs. (2), (3), and (4) we see that at low temperatures or long jump times, the line width is independent of temperature and is equal to the rigid lattice value. At high temperature or short jump times, the line width decreases exponentially with increasing temperature. The division between high and low temperatures occurs when $\tau\delta\omega_0 \sim 1$.

It has been found of much value to consider in some detail the location of the dividing temperature. To this end we make the reasonable assertion that at the onset of narrowing $\tau\delta\omega_0$ is equal to a constant, b, for all materials with like lattice structure. With less assurance, we may compare materials of different lattice structure, relying on the fact that the errors enter only logarithmically. Substituting from (3) and (4), we have

$$\delta\omega_0 a^2/12D(T_N)=b=(a^2\delta\omega_0/12D_0) \exp[E_D/T_N], \quad (5)$$

in which T_N is the "narrowing temperature." The value of b which one should use clearly depends on one's definition of the narrowing temperature. A convenient operational method for defining T_N is to extrapolate the exponential temperature dependence of the narrowed resonance towards lower temperatures and take the temperature at which it intersects the rigid lattice value. The consistency of this procedure checks very well for the lithium and sodium data of Holcomb and Norberg[1] where both E_D and D_0 are known. The lithium data yields $b=6.0$ and the sodium data $b=5.7$ in which the factor 12 appearing in Eqs. (3) and (5) has been replaced by 8 since lithium and sodium have bcc lattices. Having determined b, it is possible to predict at which temperature a resonance will narrow given the activation energy, D_0, and the rigid lattice breadth. Using Nowick's theoretical values for aluminum, namely, $D_0=0.45$ cm^2/sec and $E_D=1.43$ ev, we find $T_N \simeq 330$°C in good agreement with Seymour's data.

It is interesting to note that Seymour's analysis of his data resulted in a much smaller value of D_0 than theoretically expected. This is undoubtedly another illustration of Nowick's observation[2] that low experimental activation energies are always accompanied by low experimental D_0's. Nowick suggests that more reliable activation energies will in general be obtained by a single empirical determination of the absolute value of D than will be obtained from the relative changes in D observed over a small temperature range. The measured diffusion coefficient is converted to an activation energy by equating it to Eq. (4) into which a theoretical value of D_0 is substituted. The "narrowing" temperature notion is merely a means of applying Nowick's suggestion.

The possibility of a nonsecular dipolar contribution is easily investigated. The corresponding thermal relaxation rate represents an upper limit for the nonsecular line width. Torrey[13] has developed a complete theory of the dipolar T_1 considering in detail the effects of diffusion. The theoretical expression of Torrey is

$$(1/T_1)_{\rm dip}=7.1\gamma^4 \frac{\hbar^2 I(I+1)}{\omega_0 a^6} \frac{\psi(k,y)}{k^3}, \quad (6)$$

where $k=0.74335$ for the fcc lattice, $y=\omega_0\tau/2$, and $\psi(k,y)$ is a dimensionless function which is tabulated by Torrey. For our purpose we simply need one value of ψ, namely $\psi_{\max}=0.2906$. Evaluating (6) at 11 Mc/sec with the maximum value of ψ, we obtain $(1/T_1)_{\rm dip} \leqslant 2.90$ sec^{-1}. This is much less than the maximum electron relaxation rate of ~ 500 sec^{-1} expected near the melting point. Consequently, even the observed T_1's should not reveal a dipolar contribution.

Combining the secular dipolar contribution and both the secular and nonsecular electron contributions, we find that the observed line width in aluminum should be described by

$$(1/T_2)_{\rm obs}=(1/T_2')_{\rm dip}+(1/T_1)_{\rm obs}, \quad (7)$$

over the entire range, that is, up to the melting point. [Strictly speaking, Eq. (7) is only an approximation except for the motional narrowing region.] Furthermore, we anticipate that $(T_1)_{\rm obs}=(T_1)_{\rm elec}$, also over the entire range. At low temperatures the line width is dominated by $(1/T_2')_{\rm dip}=22\,000$ sec^{-1}. In the vicinity of 330°C the secular dipolar width should decrease rapidly until the line width is solely determined by $(1/T_1)_{\rm elec}$ which equals ~ 500 sec^{-1} near the melting point. It will be shown in Sec. IV that the data are consistent with this description except for the necessity of postulating an additional secular contribution, $(1/T_2')_x$, which is constant over the temperature range investigated and which is equal to ~ 450 sec^{-1}. The consistency of this assignment is discussed in Sec. IV.

III. EXPERIMENTAL METHODS

The spin-phase memory time and thermal relaxation time were determined by means of the spin-echo techniques of Hahn.[14] An important modification of pulsed resonance methods heretofore employed was the use of phase-sensitive detection of the nuclear signals, a technique made possible by employing phase-coherent rf pulses. For most of the measurements, the output of the phase-sensitive detector was fed to a gated integrating voltmeter quite similar to the boxcar integrator of Holcomb and Norberg.[1] The use of automatic tracking of echoes by the integrator was convenient and also

[13] H. C. Torrey, Phys. Rev. **92**, 962 (1953).
[14] E. L. Hahn, Phys. Rev. **80**, 580 (1950).

eliminated possible errors in setting the voltmeter on the echo maximum. The use of a recorder following the integrator when response times were greater than a few seconds was an invaluable aid in obtaining the utmost from the data. All measurements herein reported were made at a frequency of 11 Mc/sec which necessitates an external field of 10 kilo-oersteds. An electromagnet, some details of which have been given elsewhere[15] and which adequately met the stability requirements imposed by the phase-coherent method, was used for the measurements.

A. Phase Coherent Method

The limitations of detecting transient nuclear induction signals in the absence of an rf carrier become quite apparent when one encounters signals comparable to noise. Direct amplitude detection of the signals suffers principally for three reasons. The most important and fundamental limitation is that all integrating devices for improving signal to noise require that the noise be both positive and negative. If one is concerned with noise near, for example, 11 Mc/sec, one may well ask how plus and minus are defined. After all, any 11-Mc/sec voltage is both positive and negative. The answer to the question is that we must take an 11-Mc/sec reference. By comparison with it, we may distinguish cases where both references and "noise" are in step, hence positive (and thus negative) at the same time, from cases where the reference and "noise" are out of step, one being positive when the other is negative. That is, the plus or minus quality of noise has meaning only in terms of the phase of the noise with respect to a reference. If one uses an ordinary diode detector, and observes the output of an oscilloscope, one finds that the noise is all of one sign except when a coherent rf voltage is present, as for example, during the pulse of a large echo. If one puts the output of an ordinary diode detector into a boxcar integrator, the noise will average to zero as long as the echo is larger than noise. When the echo becomes comparable to noise, phase reference is lost, the noise becomes rectified (all of one sign) and in fact the *signal* now becomes randomly plus or minus. All attempts at integration then fail. Norberg and Holcomb[1] point out that the full potential of their boxcar integrator would only be achieved by initial phase-sensitive detection. The second difficulty with simple diode detectors is the nonlinearities which arise for small signals. The third difficulty is that even for large signals there is a correction which must be applied because the "straight line" detector response does not pass through the origin.

In the phase-coherent apparatus employed for the aluminum experiments, a stable continuously running rf oscillator supplies a cathode modulator and also furnishes a cw reference signal to the detector. The modulator output is power-amplified, and supplied to the sample coil to provide the nutating magnetic field, H_1. The nuclear signal induced in the sample coil is then amplified, added to the cw reference signal, and their *sum* is detected by a diode detector. The reference signal is adjusted to be in phase with the nuclear signal by varying the tuning of one or more intermediate tank circuits. Equality of phases was ascertained by insisting upon an induction decay which was symmetric with regard to slight shifts of the external field either side of resonance.

The requirements on magnet stability are easily examined. To do so, we write the output of the detector as

$$V=B+A(t)\cos(\gamma ht-\varphi), \tag{8}$$

in which B and A are the respective amplitudes of the references and nuclear induction voltages at the detector, h is the deviation of the external field from resonance, t is the time measured from the terminus of the exciting pulse, and φ is the phase difference between reference and nuclear signal which if adjusted as described may be assumed to be zero. During a T_1 run, an induction signal is measured at $t=30$–40 microseconds. A 2% accuracy in determination of A required that $\cos(\gamma ht)=1$ to within 2%. For aluminum nuclei a detuning $h\lesssim 0.1$ oersted is allowed. The stability requirements are much less severe for the spin-echo measurements. The same considerations which explain the echo formation also, in virtue of the π pulse, reveal that no net phase shift is produced by a static field detuning. On the other hand, a field drift of one milligauss in an echo time of three milliseconds would produce a 2% effect on the echo height.

B. General Description of the Apparatus

The over-all disposition of the electronics is shown in the block diagram of Fig. 1. The required sequences of pulses and triggers are produced by a generator in which the pertinent pulse spacings are derived from a calibrated variable audio-frequency source. The rf pulses produced in the modulator pass through a four-stage balanced power amplifier operating class C. The residual feed-through of the modulator is reduced to a tolerable level (a few hundred microvolts) in passing through the normally cut off class C stages. A symmetric rf bridge of which one arm contains the sample coil is employed to protect the receiver from the intense rf bursts and also serves to balance out the 100 microvolts residual feed-through. The peak-to-peak amplitude of the flipping magnetic field was 200 oersteds providing a $\pi/2$ nutation of the aluminum nuclear magnetization in times $\gtrsim 6$ μsec. The tuned rf amplifier consists of four similar broad-band singly tuned stages. The amplifier has a band pass of $\sim$200 kcps and an over-all gain greater than 10^5. A good bridge balance results in a receiver unblocking time of $\sim$12 μsec as illustrated in

[15] R. T. Schumacher and C. P. Slichter, Phys. Rev. **101**, 58 (1956).

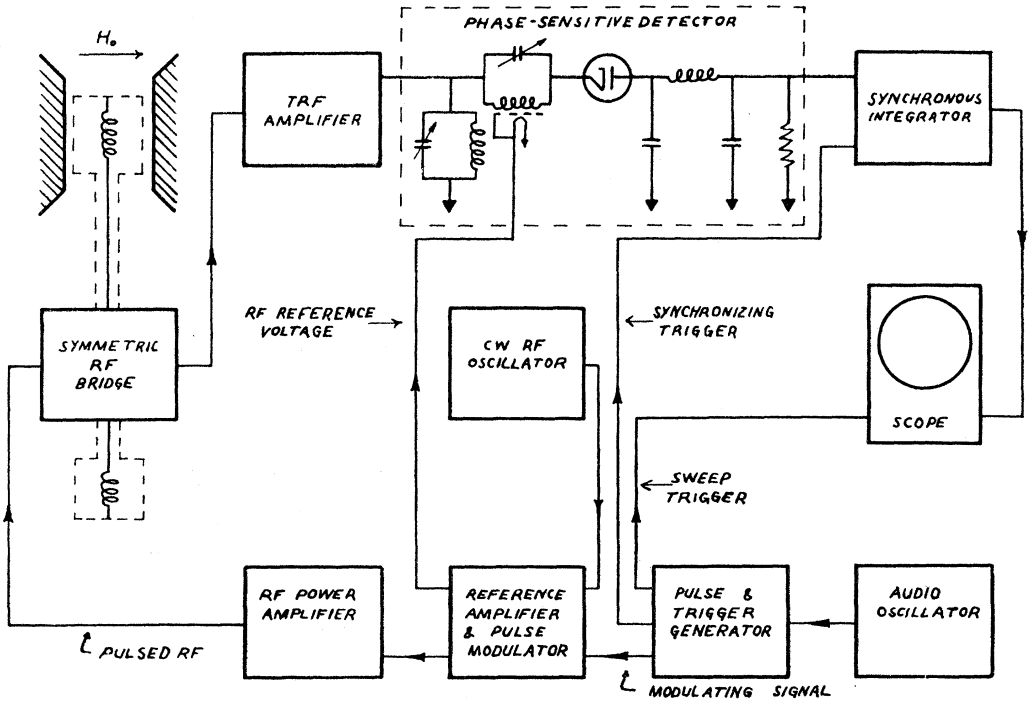

FIG. 1. Block diagram of the phase-coherent apparatus.

Fig. 2. The receiver output is viewed directly on an oscilloscope and also goes to the synchronous integrator. The integrator was useful not only as a narrow-banding device but also to provide a convenient and precise meter reading of signal heights. Figure 3 indicates the available sensitivity at the highest temperatures.

C. Rf Pulse Configurations

The broad resonances in the rigid lattice and through the initial stages of narrowing were investigated by analyzing the free induction decay succeeding a single rf pulse which nutated the nuclear magnetization through $\pi/2$ radians. The simple expedient of maximizing the induction signal served to adjust the pulse duration properly. At least ten times the thermal relaxation time was always allowed for equilibrium to be established before each measurement.

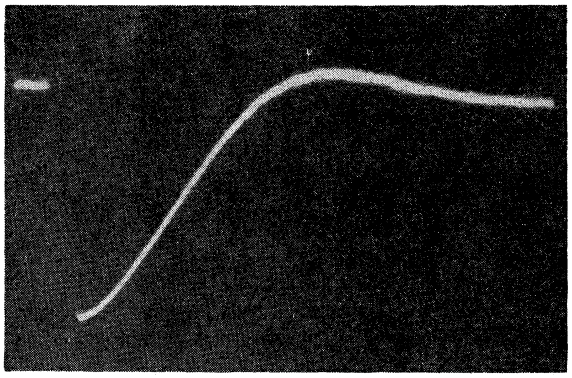

FIG. 2. Oscilloscope display of the aluminum rigid-lattice Bloch decay. The sweep length is 270 microseconds. The 18-microsecond gap in the trace represents a 6-microsecond pulse and an unblocking time of 12 microseconds.

The preponderance of line shape data was obtained by using a sequence of two rf pulses, one of duration t_1 followed a time τ later by one of length t_2. The pulses were adjusted to give nutations of $\pi/2$ and π, respectively. A pulse was said to give a π nutation if when it acted upon the spin system in equilibrium no induction signal ensued. The interval τ is equal to the period of the audio-frequency mentioned in the previous section and could be varied continuously from 50 μsec to 50 milliseconds. Theory shows that the height of the induction signal occurring at 2τ (the position of the spin echo) as a function of $t=2\tau$ is the Fourier transform of the absorption line and is to a large extent independent of the external field inhomogeneities.

The thermal recovery of the spin system was investigated by applying a π pulse followed a time τ later by a $\pi/2$ pulse. The first pulse reverses the populations of the nuclear Zeeman levels (corresponding to a heating of the spin system to the corresponding negative temperature) while the second pulse is utilized to determine the amount of recovery of the nuclear magnetization at the various succeeding times.

D. Sample and High-Temperature Probe

Initial measurements were attempted on fine powders which, it was found, would sinter at temperatures above

450°C thereby rendering them useless. All data presented below were obtained on samples consisting of 1-mil foils which were 99.99% pure. Aluminum ribbons 1–2 cm in length were placed upon a Pyrex ribbon 3 mils thick and this combination was then wound onto a small hollow ceramic tube. The resulting cylindrical roll of nominally 1-cm o.d. fitted snugly into the rf coil. The hollow tube permitted a thermocouple to be placed at the center of the sample.

The classical rf penetration depth in aluminum at room temperature and 11 Mc/sec is ~27 microns. Reasonably uniform penetration was obtained as manifested by the decay of the nuclear magnetization during the rf pulse. However, slight effects were discernible which appeared to be associated with the nonuniformity of the rf field. Specifically, the echo height was observed to vary slightly with a small detuning of the external field. A calculation following the methods of Hahn[14] revealed that a distribution in nutation frequency would produce such effects. The calculation also predicted that these spurious effects should decay with a characteristic time $T_2^*=1/\gamma\Delta H$, where ΔH is the observed line width. Consequently the resonance was always artificially broadened for the echo runs, as can be seen in Fig. 3.

The sample coil and heater were housed in a sealed copper tube 2 inches in diameter by 6 inches long. A plug of fire-brick material with a 1-inch bore 5 inches deep filled the copper housing and gave adequate thermal insulation. Fitting snugly into the bore was the heater consisting of a bifilar noninductive solenoidal winding of No. 22 Nichrome wire wound on a 3-inch length of thin-walled stainless steel tubing. One end of the housing was sealed and a flange with an O-ring groove was mounted on the other. A coaxial section consisting of a 4-inch length of thin-walled iconel tubing $\frac{1}{2}$-inch o.d. with a No. 22 copper wire as center conductor was fastened to the removable flange. The sample coil terminated the free end of the coaxial section. With the probe assembled the sample was located at the approximate center of the heater. The sealed probe when filled with dry nitrogen gas has been maintained at temperatures above 400°C for days without deterioration of its contents. Current for the heater was derived from storage batteries which held the temperature to within 1 degree centigrade for periods of more than one hour. Chromel-alumel and copper-constantan thermocouples were employed for the temperature measurements.

IV. RESULTS AND INTERPRETATION

The aluminum data of most interest are summarized in Fig. 4. Measurements which are not included in the figure extend down to room temperature in addition to points at liquid nitrogen temperature and immediately above the melting point. The rigid lattice resonance obtains below approximately 280°C. The initial stages of narrowing are characterized principally by a change in shape. The rigid-lattice Bloch decay changes smoothly and continuously from the rigid-lattice shape below 280°C to an essentially exponential decay above 360°C. Above 360°C the phase-memory time which is taken to be the time constant of the exponential decays increases sharply but levels off to an approximately constant value which is almost a factor of two less than

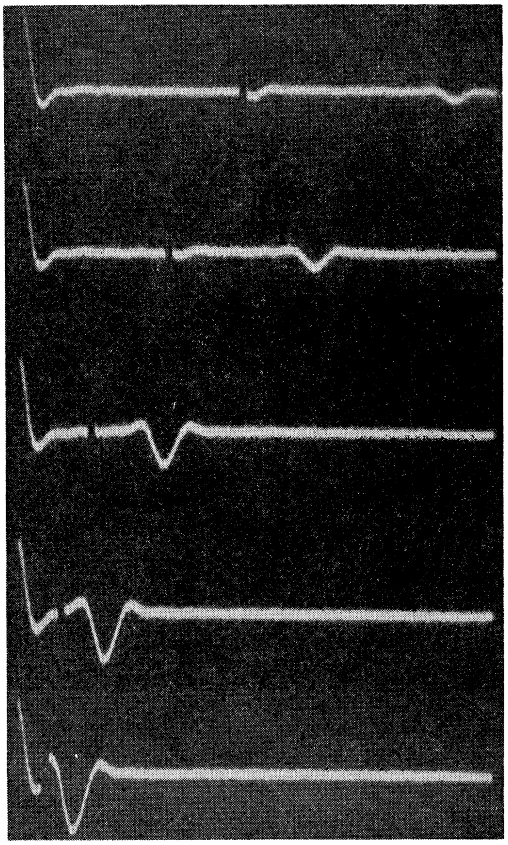

FIG. 3. Oscilloscope display of a spin-echo sequence at 625°C. The echo times are 0.4, 0.6, 1.0, 2.0, and 3.0 milliseconds.

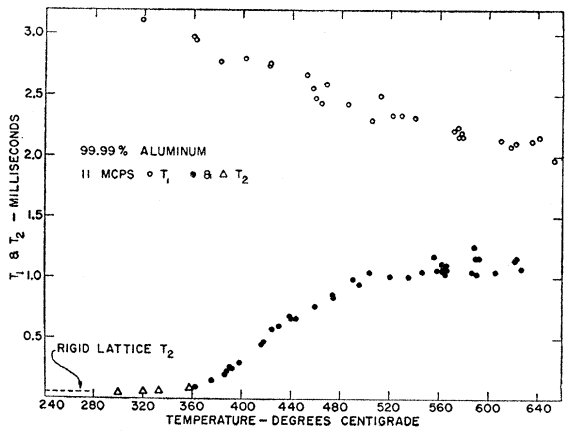

FIG. 4. High-temperature line width and thermal relaxation data in aluminum. The triangles correspond to second-moment determinations described in the text.

T_1. This feature of the data is a clear indication of a line-breadth source in addition to the nuclear dipole and conduction electron interactions. The lack of complete narrowing, given by $T_2=T_1$, is reminiscent of the lithium and sodium data.[1] Measurements in the melt give $T_2\simeq T_1\simeq 2.1$ msec. The observed thermal relaxation times follow a reciprocal temperature dependence throughout the range of experiment.

A. High-Temperature Aluminum Line Width

The rigid-lattice Bloch decay represents a pronounced departure from a Gaussian form. A "beat" which is clearly seen in Fig. 2 undoubtedly represents the same phenomenon observed in many solids by Lowe and Norberg.[16] Below 360°C there is ambiguity concerning an appropriate line-width parameter with which to describe the resonance since the shape is changing. Figure 5 gives a vivid illustration of the manner in which the narrowing proceeds in its early stages. First the overshoot diminishes and also the initial slope begins to increase slightly as illustrated by the 297°C and 329°C data of Fig. 5. At approximately 325°C the entire decay is Gaussian but at slightly higher temperatures the tail falls off less rapidly than a Gaussian. At 340°C two dependences can be seen in the decay. The initial portion varies as t^2 and the tail as t on a semilogarithmic plot. Finally at 360°C the entire decay follows an exponential. The phase-coherent apparatus

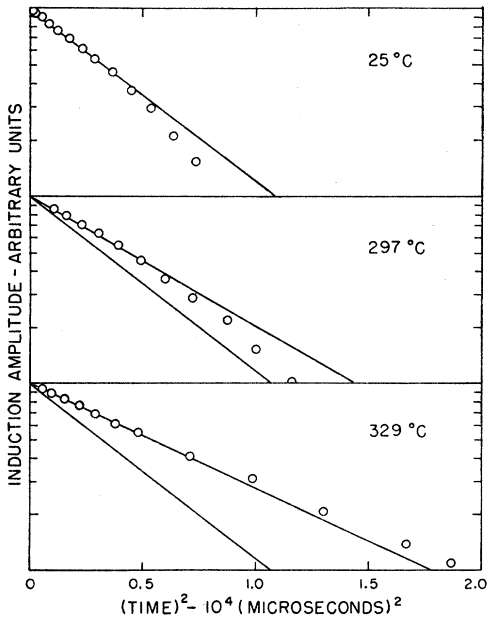

FIG. 5. Bloch decays in the intermediate region. The amplitude of the free induction signal is plotted on a logarithmic scale *versus* t^2. The lines drawn through the experimental points yield $T_2=48$, 56, and 64 microseconds. The 48-microsecond line is repeated on the lower plots.

[16] I. J. Lowe and R. E. Norberg, Phys. Rev. **107**, 46 (1957).

together with the automatic echo tracking allowed the echo decays to be determined over almost two orders of variation in echo height.

The coefficient of t^2 in the moment expansion of the Bloch decay is $\frac{1}{2}\langle\Delta\omega^2\rangle$,[16] where $\langle\Delta\omega^2\rangle$ is the mean square angular frequency deviation of the absorption. Hence the initial slope of the decay considered as a function of t^2 is directly related to the second-moment. The triangles of Fig. 4 represent second-moment determinations obtained from the straight lines drawn as in Fig. 5, using as a definition of T_2 that $1/T_2=(\langle\Delta\omega^2\rangle)^{\frac{1}{2}}$. It should be noted that the initial portion of the decays cannot be observed due to blocking of the receiver. Obtaining the initial slope from these lines involves an extrapolation in which it is assumed that the initial portion of the decays follows a Gaussian curve. The value obtained for the rigid lattice second-moment by this procedure is 9.8 ± 1.2 gauss^2. Van Vleck's[11] theoretical expression yields 7.63 gauss^2. By direct observation of the absorption, Gutowsky and McGarvey obtained 10.5 gauss^2,[11] Seymour 11.2 gauss^2,[3] and Rowland 8.7 gauss^2.[8] To be sure there is some scatter in the values but all are significantly greater than the theoretical value. The narrowing proceeds as expected except for the extra broadening which ultimately limits the line width. The magnitude of the additional broadening is not sufficient to explain the above discrepancy in the rigid-lattice breadth although there is some uncertainty due to the grossly different line shapes. A contribution founded in a combination of the pseudo-dipolar and nuclear spin exchange interactions discussed by Bloembergen and Rowland[17] is consistent with the known facts. To a good approximation these interactions will narrow concurrently with the dipolar.

Both Kubo and Tomita[6] and also Anderson[18] have shown that the second moment should be unaffected by motion. Their proof is based on the introduction of a term $\mathcal{H}_m$ into the Hamiltonian to represent the kinetic and potential energies of the nuclei. $\mathcal{H}_m$ may now be incorporated into Van Vleck's second-moment expression

$$\hbar^2\langle\Delta\omega^2\rangle=\mathrm{Tr}[(\mathcal{H}I_x-I_x\mathcal{H})^2]/\mathrm{Tr}(I_x^2),$$

where I_x is the total x component of nuclear spin, and $\mathcal{H}$ is now the total Hamiltonian. Since $\mathcal{H}_m$ commutes with I_x, it drops out of the expression for $\langle\Delta\omega^2\rangle$.

In contrast to this view is the work of Pake and Gutowsky, Andrew and Eades,[19] and others who have studied the effect of motion on the second moment of resonance lines. They compute the second moment by Van Vleck's expression, but they modify the angular factors to take account of the motion. Thus, in the case of the coupling of a pair of nuclei undergoing rapid rotation, they use for the dipolar coupling the value

[17] N. Bloembergen and T. J. Rowland, Phys. Rev. **97**, 1697 (1955).

[18] P. W. Anderson, J. Phys. Soc. (Japan) **9**, 316 (1954).

[19] For a good review, see E. R. Andrew, *Nuclear Magnetic Resonance* (Cambridge University Press, Cambridge, 1955).

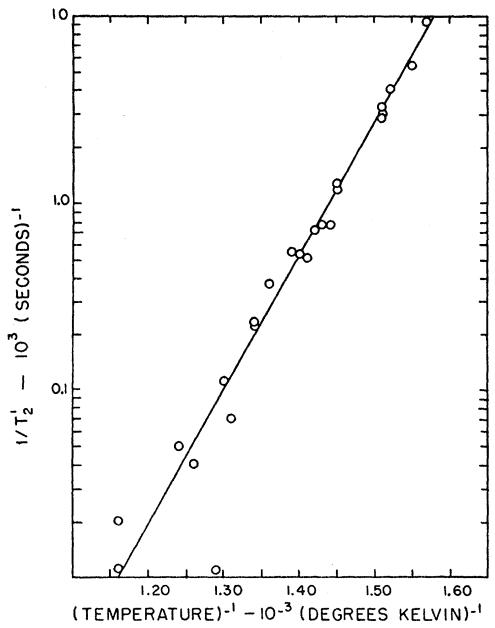

FIG. 6. The secular dipolar width *versus* the reciprocal of the absolute temperature. The straight line corresponds to an activation energy $E_D=1.41$ ev.

obtained by averaging over the rotation. Consequently, although $\mathcal{H}_m$ does not appear explicitly in their expression for the second moment, in agreement with Anderson, and Kubo and Tomita, it appears implicitly in the choice of angular variables.

Over the range in which we feel the initial slope may be obtained reasonably reliably, we observe a decrease of approximately a factor of two in second moment, as illustrated in Fig. 5. Our results are therefore in agreement with the second view, and support the contention that the second moment *is* affected by motion.

The activation energy for self-diffusion is obtained by fitting the narrowed dipolar width (i.e., in the Lorentzian region) to an exponential temperature dependence. The decomposition of the line width,

$$(1/T_2)_{\text{obs}}=(1/T_2')_{\text{dip}}+(1/T_2')_x+(1/T_1)_{\text{obs}}, \quad (9)$$

permits, as will be seen, the dipolar contribution to be determined over the range ~360°C to 500°C. The term $(1/T_2')_x$ represents a secular contribution of unknown origin which is assumed responsible for the fact that $(T_2)_{\text{obs}}$ does not narrow all the way to T_1. Only the data above 360°C are utilized since only in this region is there no ambiguity in the line shape. The justification of Eq. (9) stems from the belief that $T_1)_{\text{obs}}=T_1)_{\text{elec}}$, as supported by both the magnitude of T_1 and its temperature dependence.

The x interaction dominates the line breadth above ~520°C. At these temperatures the dipolar term can be dropped from the right-hand member of (9). Hence, subtracting the T_1 term from the observed width leaves the secular contribution of the x interaction. In this manner it is found that $(1/T_2')_x$ is essentially independent of temperature with a mean value of $(T_2')_x=2.3$ msec. It is assumed that the constancy of $(T_2')_x$ is maintained in the region in which the dipolar width dominates the observed width. With this assignment the dipolar width can be determined by Eq. (9). The result of this procedure is summarized in Fig. 6 in which $(1/T_2')_{\text{dip}}$ is plotted on a logarithmic scale *versus* $1/T$. The accuracy at the highest temperatures is of course quite poor because of the large subtractions which are necessary. While there is scatter in the points, a reasonably good exponential temperature dependence is found in accord with theoretical expectations. The activation energy which is obtained from the straight line fitted to the points plotted in Fig. 6 is $E_D=1.4\pm0.1$ ev. The assigned uncertainty represents the scatter in the points and does not include possible uncertainties in the procedure.

The subtraction which was applied to the T_2 data of Fig. 4 in order to obtain Fig. 6 is quite large. However, there is no doubt that another line width contribution is present and must be taken into account. Two limiting assignments, $(T_2')_x=2.70$ and 2.15 msec, which seem to bracket the extra broadening, were also tried. The resulting data when plotted as in Fig. 7 yield activation energies of ~1.25 ev and ~1.53 ev, respectively. The 2.70-msec assignment (1.25 ev) leaves definite curvature in the plot. There is no consistent curvature with the larger subtraction. When only the electron T_1 contribution is removed from the raw data, the initial slope indicates $E_D\gtrsim1.25$ ev and, of course, there is a pronounced curvature.

Extrapolating the straight line in Fig. 6 to the rigid-lattice width of 23×10^3 sec^{-1} (not visible in Fig. 6)

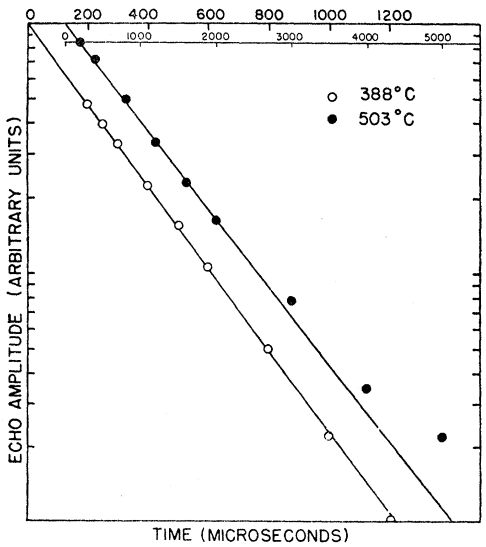

FIG. 7. Typical decays of the transverse nuclear magnetization for the narrowed aluminum resonance. The straight lines represent $(T_2)_{\text{obs}}=265$ and 1110 microseconds.

yields a narrowing temperature of 340°C. This is in excellent agreement with the value 330°C predicted in Sec. II on basis of the alkali-metal resonance data and Nowick's estimates for E_D and D_0 in aluminum. Thus we have consistency in that the energy determined from the narrowing temperature agrees with the energy derived by the slope method. The activation energy for self-diffusion determined in this research is 1.40 ± 0.1 ev.

Recent quenching experiments on aluminum have been reported by Bradshaw and Pearson.[20] They obtain 0.76 ev for, E_f, the energy of formation of a vacancy which they determine from the dependence of the quenched-in electrical resistance on the quench temperature. They further interpret the annealing of the quenched-in resistance from which they obtain 0.44 ev for, E_m, the energy of vacancy migration. Adding E_f to E_m they get 1.2 ev for the activation energy of self-diffusion, a value which disagrees somewhat with the result of this research (1.4 ± 0.1 ev) and likewise with Nowick's prediction 1.43 ev. The reason for the disagreement is not at present known. DeSorbo and Turnbull[21] have also reported on quenching experiments in aluminum. They give $E_m=0.52$ ev and $E_f=0.79$ ev for the respective energies as determined from their measurements, giving $E_D=1.31\pm0.08$ ev. Although our value is higher than theirs, the disagreement is not outside of the assigned errors and is probably not significant.

B. Discussion of the Additional Broadening

The decay of the transverse nuclear magnetization above approximately 450°C, as manifested by the echo decay, exhibits a slight departure from a simple exponential. Between 360°C and 450°C, only exponential decays were observed. The magnitude and nature of the difference is illustrated in Fig. 7 by the 503°C data. The effect which is just barely resolved represents approximately one percent of the initial echo height, but was consistently present above 450°C and for this reason it is considered real. Since the deviation from an exponential was observed only in the region in which the line width is dominated by the extra broadening, it is assumed to be characteristic of the extra broadening.

A spurious broadening caused by diffusion through external field gradients can be observed in an echo experiment. It has been shown[14,22] that this effect modulates the echo envelope with a factor $\exp(-kt^3)$, in which k is a constant which depends on the diffusion coefficient and the field gradients. Since such a term causes the echo amplitude to decrease more rapidly than a simple exponential, the opposite to that which is observed, we can eliminate this as a possible explanation of the broadening.

Surface effects can be easily dismissed as cause of the extra broadening. These effects depend upon appreciable diffusion across sample grains in times comparable to T_1 and T_2. Examination of etched 99.99% aluminum foils which were used in this research revealed the average grain diameter to be ~30 microns (slightly larger than the foil thickness). The mean time for an atom to diffuse a distance L is $t\simeq\frac{1}{2}(L/a)^2\tau$, in which a is the lattice constant and τ the mean time between jumps. Using $\tau=10^{-8}$ sec, appropriate for temperatures near the melting point on basis of the constants measured in this work, and $L\sim30$ microns yields $t\sim10^2$ sec whereas $T_2<T_1\simeq2.3$ msec. It is concluded that the particle size is large enough to exclude surface effects in these experiments. Consistent with this conclusion is the fact that no additional broadening is observed in the melt, which is contrary to that which is expected for surface effects since the diffusion increases upon melting.

The fact that $(T_2)_x$ is independent of temperature suggests that the broadening is not motionally narrowed. It cannot be caused by inhomogeneous magnetic fields due to paramagnetic impurities because the spin-echo does not decay as a result of static magnetic field inhomogeneities.

The remaining possibility is a coupling of the nuclear quadrupole moment to lattice strains produced by foreign atoms, vacancies, interstitials, dislocations, or elastic stress.

One might suppose that just as the echo method causes a refocusing of static magnetic interactions, likewise it would refocus a static quadrupolar interaction. However, it is a simple matter to show that a $\pi/2$—π pulse sequence does not refocus a first-order static quadrupole broadening, and that in fact the echo envelope has the same shape as the free induction decay in a perfectly homogeneous magnet.

In first order, a quadrupole interaction does not affect the frequency of the $m=-\frac{1}{2}$ to $m=+\frac{1}{2}$ transition. The other transitions are shifted. For the case of lattice strains which are not homogeneous, a distribution in shifts is present, giving rise to a line broadening.[23] The echo envelope, being the transform of the absorption line, will therefore have components which die out and a persistent component whose amplitude is 9/35 of the maximum induction signal. For our case, the rapid spin-lattice relaxation will greatly complicate the decay, but the general feature of a persistent tail at long times should remain. A quadrupolar coupling therefore seems to be a good possibility. Which of the possible sources of strain is responsible?

The quadrupole interaction with vacancies has been discussed by Bloembergen.[23] He points out that one might see direct vacancy effects in metals only near the

[20] F. J. Bradshaw and S. Pearson, Phil. Mag. **2**, 570 (1957).
[21] W. DeSorbo and D. Turnbull, Bull. Am. Phys. Soc. Ser. II, **2**, 262 (1957), and private communication.
[22] H. Y. Carr and E. M. Purcell, Phys. Rev. **94**, 630 (1954).
[23] N. Bloembergen, in *Report of the Bristol Conference on Defects in Crystalline Solids, 1954* (Physical Society, London, 1954).

melting point where the concentration approaches perhaps $\sim 10^{-3}$. The correlation time for a vacancy interaction is so short that $(T_2)_{\text{vac}} = (T_1)_{\text{vac}}$. Since only a T_2 contribution was observed for the x interaction, a vacancy mechanism is effectively ruled out.

Since the additional breadth was essentially constant, we assume that the responsible interaction is in its unnarrowed form. Accordingly the condition

$$\tau_x(1/T_2')_x \gtrsim 1, \tag{10}$$

in which τ_x is the correlation time characteristic of the x interaction and $(T_2')_x = 2.3$ msec, should hold up to the melting point.

It is reasonable to assume that the x interaction varies from point to point in the sample, being positive in some places and negative in other. (Such would be the case for a quadrupolar coupling with dislocations or impurities.) If a nucleus were to diffuse a distance sufficiently great for the interaction to change sign, we have the possibility of motional narrowing. The time for a nucleus to diffuse such a distance, L, would then be the correlation time τ_x since the interaction would be coherent for shorter times. We find that τ_x is given in terms of the lattice constant, a, and the mean time between jumps, τ, by

$$L^2 \simeq \tfrac{1}{2} a^2(\tau_x/\tau). \tag{11}$$

From the narrowing of the dipolar width, we have $\tau = 10^{-8}$ sec near the melting point. Combining (10) and (11) and substituting this value of τ results in the inequality

$$(L/a)^2 \gtrsim 3 \times 10^4. \tag{12}$$

We thus have an upper limit to the concentration of sources responsible for the extra broadening. The equality sign in (12) would correspond to the x interaction being on the verge of narrowing at the melting point.

A quadrupole perturbation due to the strain field surrounding a dislocation produces a line breadth $(1/T_2')_x \simeq \delta\omega_{\text{dis}}(a/L)$, where L is the mean dislocation spacing and $\delta\omega_{\text{dis}}$ is the strength of the interaction for a nucleus adjacent to the dislocation. Substituting from (12) gives $\delta\omega_{\text{dis}} \gtrsim 10^5$ sec^{-1} which is easily satisfied. The experiments of Rowland[24] on quadrupole effects in aluminum caused by foreign atoms indicate that several Mc/sec is not unreasonable for the nearest neighbor interaction. The strain near a dislocation is presumably of the same order or larger than that near a representative foreign atom. Condition (12) requires the dislocation density in the bulk of the sample to be less than $\sim 5 \times 10^{12}$ line/cm^2. A larger nearest neighbor interaction which is eminently reasonable allows a corresponding smaller dislocation density.

The dilution of sources dictated by (12), coupled with the short-range strain field surrounding a chemical impurity, necessitates what we feel is an impractically large interaction strength in order to account for the extra broadening through foreign atoms. In particular, a nearest neighbor interaction $\delta\omega_{\text{chem}} \gtrsim 10^9$ sec^{-1} is indicated. We conclude that dislocations are a likely candidate for the extra broadening. Long-range strains which might encompass entire crystal grains also fit the above picture. A partial relaxation of the strain could account for the decrease in line width upon melting. A systematic study of effects of strain and impurities on $(T_2)_x$ would be most interesting.

C. Thermal Relaxation in Aluminum

The nuclear spin thermal relaxation caused by the conduction electrons in metals has been calculated by Korringa[7] and others. The relaxation rate which results from the Fermi contact term is

$$(1/T_1)_{\text{elec}} = (\pi kT/\hbar) v_0^2 N^2(E_f) C^2 E_{\text{hf}}^2, \tag{13}$$

in which v_0 is the atomic volume, $N(E)$ is the density of states, E_f is the Fermi energy, E_{hf} is the hyperfine constant for the free atom, and C is the ratio of the electron density at the nucleus in the metal to the density at the nucleus in the free atom suitably averaged over the Fermi surface. According to (13), $(T_1)_{\text{elec}}$ is proportional to the absolute temperature. This dependence originates in the electron statistics and is also obtained for the T_1 contribution which may be caused by the neglected terms of the Hamiltonian. The contact part of the electron interaction also gives rise to a paramagnetic shift $(\Delta H/H_0)$, called the Knight shift, of the metal nuclear resonance. As Korringa has shown,[7] the Knight shift and electron T_1 contribution are related:

$$(T_1)_{\text{elec}}(\Delta H/H_0)^2 = (h/4\pi kT)(\gamma_e/\gamma_n)^2, \tag{14}$$

where γ_e and γ_n are respectively the gyromagnetic ratios of the electron and nucleus. The conduction electron Hamiltonian has been discussed extensively[1,8,25] with regard to the nuclear T_1 contribution, the Knight shift, and the Korringa relation.

The experimental accuracy was such that above 300°C the thermal recovery could be observed over a time equal to five characteristic times. For the broad resonances below 300°C the precision of the T_1 data was limited by the accuracy to which the field could be set to exact resonance. No deviation from a pure exponential recovery was ever detected. The experimental relaxation times are summarized in Fig. 8. Included on the graph are low-temperature high-field determinations by Anderson and Redfield[26] and by Hebel and Slichter[27] in addition to the results of the present research. It is immediately noted that T_1 in aluminum quite accurately follows the predicted

[24] T. J. Rowland, Acta Met. **3**, 74 (1955).

[25] N. Bloembergen and T. J. Rowland, Acta Met. **1**, 731 (1953).

[26] A. G. Anderson and A. G. Redfield (to be published).

[27] L. C. Hebel and C. P. Slichter (to be published).

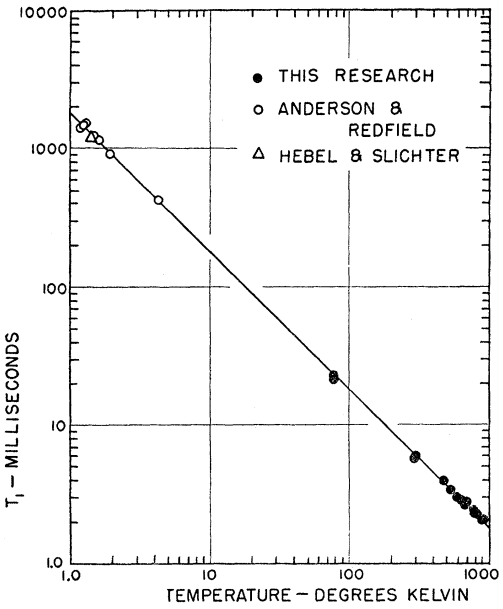

FIG. 8. Thermal relaxation time in aluminum *versus* the reciprocal temperature. The line describes $(T_1T)=1.85$ sec °K.

temperature dependence over the range ~1°K to ~930°K.

The absolute value of $(T_1)_{\text{elec}}$ per se and relative to the Korringa relation has been reviewed recently by Redfield[8] for aluminum. A general survey has been given by Pines.[28] Using the experimental Knight shift $\Delta H/H_0=0.161\times10^{-2}$,[11] the Korringa relation predicts $(T_1T)=1.50$ sec °K. The straight line of Fig. 8 corresponds to $(T_1T)=1.85$ sec °K. Ignoring correlation effects (both nuclear and electron), the Korringa relation is expected to be a possible overestimate of the electron T_1, since it neglects the other terms in the Hamiltonian which contribute to the relaxation but produce zero shift in cubic metals. Correlation effects, on the other hand, will cause the Korringa relation to predict low values of T_1.[1,8,28] The Korringa relation also yields lower T_1's than empirically observed in copper[8,9] and in lithium, sodium, and rubidium.[1] Measurements on metallic tin during the course of the present experiments gave $T_1=700\pm50$ microseconds at liquid nitrogen temperature, which also is larger than predicted by the Korringa relation.

[28] D. Pines, in *Solid-State Physics*, edited by F. Seitz and D. Turnbull (Academic Press, Inc., New York, 1955).

IV. CONCLUSIONS

Extensive and precise data have been obtained on the high-temperature aluminum resonance. The line narrowing which occurs at 330°C and which has been previously reported and interpreted by Seymour[3] has been re-examined in detail. Seymour determined an activation energy $E_D=0.9$ ev for self-diffusion in disagreement with Nowick's prediction of $E_D=1.43$ ev. However, the "narrowing temperature" indicated by Seymour's data is in accord with Nowick's prediction. The T_2 data obtained in the present experiments reveal an unexpected high-temperature line width which inhibits complete narrowing of the aluminum resonance. Fortunately, the additional line breadth manifests a simple temperature dependence, namely, it is constant. The activation energy determined by the temperature dependence of the narrowing dipolar width depends sensitively on the assignment for the additional line width. Two extreme assignments give $E_D=1.25$ and 1.53 ev. The result of the present investigation is $E_D=1.4\pm0.1$ ev determined from the best fit of the narrowed dipolar width and from the narrowing temperature.

Thermal relaxation times T_1 measured in this research together with other determinations at very low temperatures indicate that T_1 is proportional to the reciprocal of the absolute temperature from ~1°K to ~930°K, with $(T_1T)=1.85$ seconds-degrees Kelvin to within 4%.

The feasibility and practicability of phase-coherent pulsed nuclear resonance techniques have been demonstrated. The phase-coherent techniques greatly extend the range of pulsed nuclear resonance methods heretofore employed and at the same time allow significantly greater precision. The success of the high-temperature aluminum experiments is in large measure a direct result of the coherent rf apparatus.

ACKNOWLEDGMENT

It is a pleasure to acknowledge the many valuable contributions to the development of the phase coherent equipment made by Dr. L. C. Hebel.

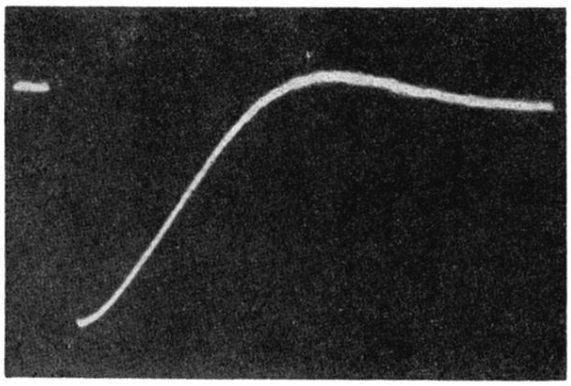

FIG. 2. Oscilloscope display of the aluminum rigid-lattice Bloch decay. The sweep length is 270 microseconds. The 18-microsecond gap in the trace represents a 6-microsecond pulse and an unblocking time of 12 microseconds.

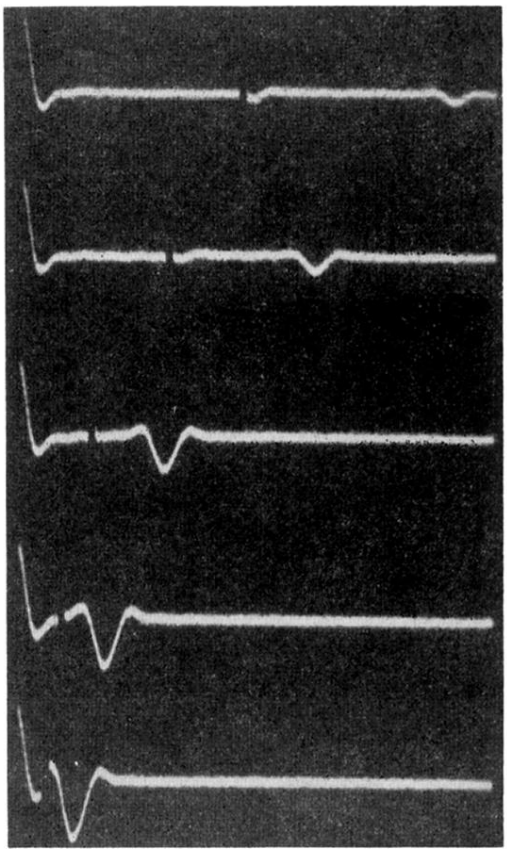

FIG. 3. Oscilloscope display of a spin-echo sequence at 625°C. The echo times are 0.4, 0.6, 1.0, 2.0, and 3.0 milliseconds.